Computer simulation of solid–liquid coexistence in binary hard sphere mixtures

By W. G. T. KRANENDONK and D. FRENKEL

FOM Institute for Atomic and Molecular Physics, PO Box 41883,
1009 DB Amsterdam, The Netherlands

We present the results of a computer simulation study of the solid–liquid coexistence of a binary hard sphere mixture for diameter ratios in the range $0.85 \leqslant \alpha \leqslant 1.00$. For the solid phase we only consider substitutionally disordered FCC and HCP crystals. For $0.9425 < \alpha < 1.00$ we find a solid–liquid coexistence curve of the 'spindle' type. For $\alpha = 0.9425$ this becomes an azeotropic and for $\alpha = 0.875$ a eutectic diagram. We compare these results with the predictions of the density functional theory of Barrat, Baus and Hansen. We observe that the density functional theory accurately predicts the point where the spindle diagram transforms into an azeotrope. However, the density functional theory differs from the simulation results on a number of counts. The greatest differences between computer simulations and theory are that the changeover from an azeotropic to a eutectic diagram is found to occur at $\alpha = 0.875$, rather than at the predicted value of $\alpha = 0.92$, that the density difference between the solid and the liquid at liquid–solid coexistence is found to have a minimum as a function of the mole fraction of the large spheres, while density functional theory predicts a maximum, and finally that the solubility of large spheres in a solid mixture of small spheres is much larger than predicted.

1. Introduction

One of the key problems in statistical mechanics is to obtain a simple yet reliable estimate of the melting point of an atomic or molecular solid for which the intermolecular potential is known. In recent years, several authors have applied density functional theory to compute the melting point of atomic solids (for a review, see [1]). On the whole it appears that density functional theory is quite successful (although not entirely without flaws) in describing the melting of atomic systems. A case where density functional theory has been applied with considerable success is in the description of the melting transition of the hard sphere system. For this system second-order density functional theory predicts [2] that at coexistence $\phi_f = 0.51$, $\phi_s = 0.56$ and $PV_0/NkT = 11.2$, which should be compared with the simulation results of Hoover and Ree [3]: $\phi_f = 0.494$, $\phi_s = 0.545$ and $PV_0/NkT = 8.27$ (± 0.13). N/V_0 is the density of regular close packing of the hard sphere solid, ϕ is the volume fraction occupied by the spheres and the subscripts s and f refer to the solid and fluid phases respectively. In fact, very recently, Baus and Lutsko [4] have developed an improved density functional theory that yields very nearly quantitative agreement with the simulation data of Hoover and Ree, namely $\phi_f = 0.495$, $\phi_s = 0.545$ and $PV_0/NkT = 8.41$.

Encouraged by the good results obtained with density functional theory for the pure (monodisperse) hard sphere system, several authors have recently considered extensions of the second-order theory to polydisperse systems. In particular, the phase diagram for binary mixtures of nearly monodisperse hard spheres has been calculated

by Barrat, Baus and Hansen [5] and Smithline and Haymet [6]. Barrat *et al.* [5] only considered the melting behaviour of substitutionally disordered FCC lattices. Smithline and Haymet [6] also considered crystalline phases with long-range substitutional order, but found these to be only metastable. The calculations in [5, 6] suggest that a change in the diameter ratio α of the spheres of only 15% has a dramatic effect on the phase diagram. In [5, 6] it was found that the melting curve changes from spindle-like close to $\alpha = 1$ through azeotropic below $\alpha = 0.94$ to eutectic for $\alpha < 0.92$.

The first numerical study of the melting point of a monodisperse three-dimensional solid was published over 20 years ago [3]. Surprisingly, prior to our work no simulation study has (to our knowledge) been reported on solid–liquid coexistence in binary mixtures, even though fluid binary mixtures have been studied extensively by simulation. In the simulations of binary hard sphere mixtures by Jackson, Rowlinson and van Swol [7] spontaneous solidification was observed, but no attempt was made either to determine the structure of the resulting phase or to locate the coexistence point.

The first simulation study of the melting curve of a solid solution was recently reported by us [8]. The results in [8] were restricted to a hard sphere mixture with a diameter ratio $\alpha = 0.90$. In the present paper we extend these simulations to a range of diameter ratio $1.0 \geqslant \alpha \geqslant 0.85$. Using these data, we are able to locate the points where qualitative changes in the phase diagram take place.

In what follows we shall use the subscripts L and S to refer to large and small spheres respectively. α denotes the ratio of diameters of the smaller sphere to that of the larger one, while X is defined as the mole fraction of the large particles.

2. Simulations

Equation-of-state data for the hard sphere mixtures were obtained by both constant-pressure Monte Carlo (*NPT*–MC) and conventional molecular dynamics simulations. To improve the sampling over the configuration space, we included Monte Carlo trial moves in which an attempt was made to permute a large and a small particle chosen at random. These particle permutations were performed both in the MC (typically, once every cycle) and the MD runs (typically, one permutation per 100 collisions). Clearly, these particle swapping moves make our MD simulations non-deterministic. For our purpose this was not serious, since we did not attempt to compute transport properties.

For diameter ratios α close to unity the acceptance of particle swapping moves is relatively high. For example, at a packing fraction $\phi = 0.5760$, a mole fraction $X = 0.5$ and a diameter ratio $\alpha = 0.90$, 45% of all attempted particle swaps in the solid are accepted. However, for a diameter ratio $\alpha = 0.85$ at the same composition and packing fraction the acceptance of particle swapping moves has been reduced to only 3% [9].

Particle swapping moves are particularly important for simulations of crystalline solids where diffusion is negligible. Without particle interchanges, the initial distribution of large and small particles over the lattice would effectively be frozen during the entire length of the simulation.

In our simulations of the solid phase we initially prepare the system in a face centred cubic (FCC) lattice without defects or vacancies: the large and small particles are initially distributed randomly over the lattice sites. However, during the

equilibration run correlations in the particle positions may build up. Cubic periodic boundaries conditions are used in all simulations. If we consider this system as a sample drawn from an infinite lattice, we may view the process of interchanging particles as a technique that allows us to take different samples from the infinite lattice. However, since we keep the total number of small and large spheres in the simulation box constant, we do neglect concentration fluctuations with a wavelength larger than the box size.

The equation-of-state data for both the liquid and the solid mixtures were obtained in simulations on a system containing 108 particles. In the Monte Carlo simulations the system was equilibrated for some $(0\cdot5-1) \times 10^4$ cycles (i.e. trial moves per particle). The actual production runs took some $1\cdot5 \times 10^4$ MC cycles. In the MD simulations the system was equilibrated during $(0\cdot6-1) \times 10^5$ collisions. The thermodynamic data of interest were collected over the next $(3-4) \times 10^5$ collisions. In all cases the initial configuration for a simulation was the final, well equilibrated, configuration of a previous run at an adjacent state point. Again, more details can be found in [9].

For the hard sphere mixture with a diameter ratio $\alpha = 0.95$ we computed the equation-of-state of the fluid at six different compositions ($X = 0 (= 1), 0\cdot2, 0\cdot4, 0\cdot5, 0\cdot6$ and $0\cdot8$). The fluid branch for $\alpha = 0\cdot90$ was computed at seven different compositions: $X = 0 (= 1), 0\cdot1, 0\cdot2, 0\cdot4, 0\cdot5, 0\cdot6$ and $0\cdot8$, and for $\alpha = 0\cdot85$ at six different compositions: $X = 0 (= 1), 0\cdot2, 0\cdot4, 0\cdot5, 0\cdot6$ and $0\cdot8$. The equation of state of the solid was computed at six different compositions for $\alpha = 0\cdot95$ and at nine different compostion for $\alpha = 0\cdot90$ and $0\cdot85$. Typically we computed some 10–15 points on every solid branch and 25 points per fluid branch.

To handle this very large amount of data (more than one thousand state points), we used a fitting procedure in which we expressed the compressibility factor as an analytical function of X, α and ϕ. This analytical function was constructed such that all the known symmetries of the thermodynamic variables were built in. Details can be found in [9].

The second step in the determination of the phase diagram is the calculation of the Gibbs free enthalpy in both the liquid and the solid. The basic idea is that we need to construct a reversible path between a reference state of known Gibbs free enthalpy and the thermodynamic state for which we want to know this quantity. For the liquid we can directly apply thermodynamic integration [10]. For the solid state accurate values of the free energy for the monodisperse FCC lattice have been calculated by Frenkel and Ladd [11] at two different densities. We have employed two independent methods to relate the free energy of a FCC solid solution at an arbitrary mole fraction X to that of the monodisperse solid. The first technique is a particle swapping method, similar in spirit to the Widom particle insertion method [10]. The difference in free energy between a system of N_1 small particles and N_2 large particles and a system of $N_1 - 1$ small particles and $N_2 + 1$ large particles at the same volume fraction follows from the ratio of the acceptances of virtual trial moves. The second method to measure the free energy of a solid solution uses a direct thermodynamic integration scheme. In this method we start with a solid solution of equal-sized particles at mole fraction X. We thereupon compute the reversible work needed to change the diameter ratio of the particles from 1 to α. The conjugate 'force' to a change in α is easily computed in a molecular dynamics simulation. These techniques are discussed in detail in [12].

In order to locate the melting curve in a binary mixture of species L and S, we must know the pressure and the chemical potentials of the individual species in both phases.

The latter quantities are most easily determined from the molar Gibbs free enthalpy $G = X\mu_L + (1 - X)\mu_S$ in combination with the relation

$$\mu_L - \mu_S = \left(\frac{\partial G}{\partial X}\right)_{N_S + N_L, P, T}. \tag{1}$$

The melting curve follows from the conditions

$$\mu_{L,s} = \mu_{L,f}, \qquad \mu_{S,s} = \mu_{S,f}, \qquad P_s = P_f, \qquad T_s = T_f.$$

The equality of temperature is not in fact an independent condition, since for hard core systems the pressure and temperature are proportional.

The phase diagrams described in this paper were obtained by the following procedure: first we fitted more than 500 liquid state points to an empirical function, which relates the compressibility factor of ϕ, X and α [9]. The same fitting procedure was used to obtain an analytical expression for almost 500 solid state points. The Gibbs free enthalpy for the liquid was obtained from the polynomial fit for the liquid by standard thermodynamic integration. For the solid state the polynomial fit for the solid was combined with the results of two different methods, which calculate the free energy difference between a mixture and a monodisperse reference system [12], to obtain the Gibbs free enthalphy of the solid as a function of α, X and the pressure.

Knowing the Gibbs free enthalphy of the liquid and the solid as a function of X at constant pressure and diameter ratio α, we apply the double tangent construction to obtain the compositions of the coexisting liquid and solid phase. Demixing in the solid can be determined by applying the double tangent construction to the Gibbs free enthalpy of the solid at constant pressure and diameter ratio α.

3. Results

3.1. *Phase diagrams*

Figures 1–6 show the phase diagrams for binary mixtures of hard spheres with diameter ratio in the range of $0.85 \leqslant \alpha \leqslant 1.0$ as obtained by the present simulations. Note that in all these figures our results for the melting point of the monodisperse hard sphere system, $\phi_s = 0.546$, $\phi_f = 0.493$, $PV_0/Nk_BT = 8.29 \pm (0.06)$, agree very well with the Hoover and Ree results: $\phi_s = 0.545$, $\phi_f = 0.494$ and $PV_0/Nk_BT = 8.27$ (± 0.13).

The most remarkable feature of the freezing of a binary hard sphere mixture is the rapid change of the nature of the phase diagrams as the spheres become increasingly dissimilar: by lowering the diameter ratio from the monodisperse system to a system with a diameter ratio $\alpha = 0.85$, we obtain three different kinds of phase diagrams, a spindle, an azeotropic and an eutectic diagram. This behaviour is in qualitative agreement with the prediction of density functional theory [5].

A more detailed comparison with this density functional theory [5] is provided by figures 1, 4 and 6. Figure 1 shows the results of our calculation and the results from this theory for a diameter ratio $\alpha = 0.95$. The qualitative agreement between theory and simulation is striking. In particular, the computer simulations confirm the spindle-type phase diagram predicted theoretically. Moreover, theory and simulation are in fair agreement about the width of the spindle (i.e. about the compositions of the coexisting phases). Note, however, that there is a large discrepancy between the coexistence pressure found in the simulations and the value predicted theoretically. Actually, this problem is not confined to *binary* systems: even for a monodisperse
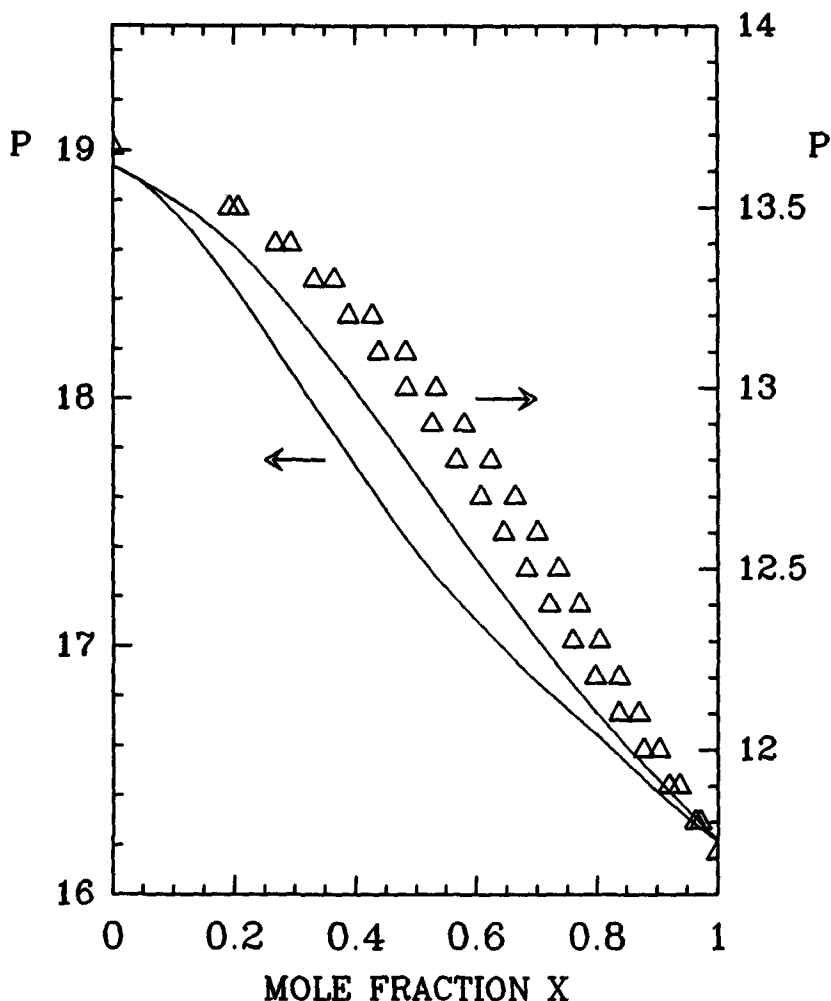
Figure 1.   Phase diagram of binary hard sphere mixture for a diameter ratio $\alpha = 0.95$. Triangles ($\triangle$) represent the results obtained computer simulations. The full line gives the theoretical prediction [5]. Because of the large discrepancy between the melting pressure of monodisperse hard spheres obtained by computer simulation and density functional theory, the ordinate axis for the coexistence pressures predicted by density functional theory (left) has been scaled and shifted with respect to the pressure axis for the simulation results (right). The pressure is expressed in units of $k_B T/\sigma_L^3$, where σ_L is the diameter of the larger sphere. The arrows in the figure indicate the labelling of the axes.

system the compressibility relation, which was used in [5], resulted in a 30% over-estimate of the coexistence pressure [2]. In view of the better agreement reported in [4], this discrepancy is not an inherent defect of density functional theory.

For $\alpha = 0.90$ (figure 4) density functional theory predicts that the phase diagram should exhibit an eutectic point. However, no such behaviour is observed in our simulations (see figure 4). Rather than a two-phase region with an eutectic point at $X \approx 0.13$, we observe a phase diagram with an azeotropic point at $X \approx 0.22$.

Finally, the diagrams for $\alpha = 0.85$ are given in figure 6. Both computer simulations and density functional theory find an eutectic diagram, although there are a
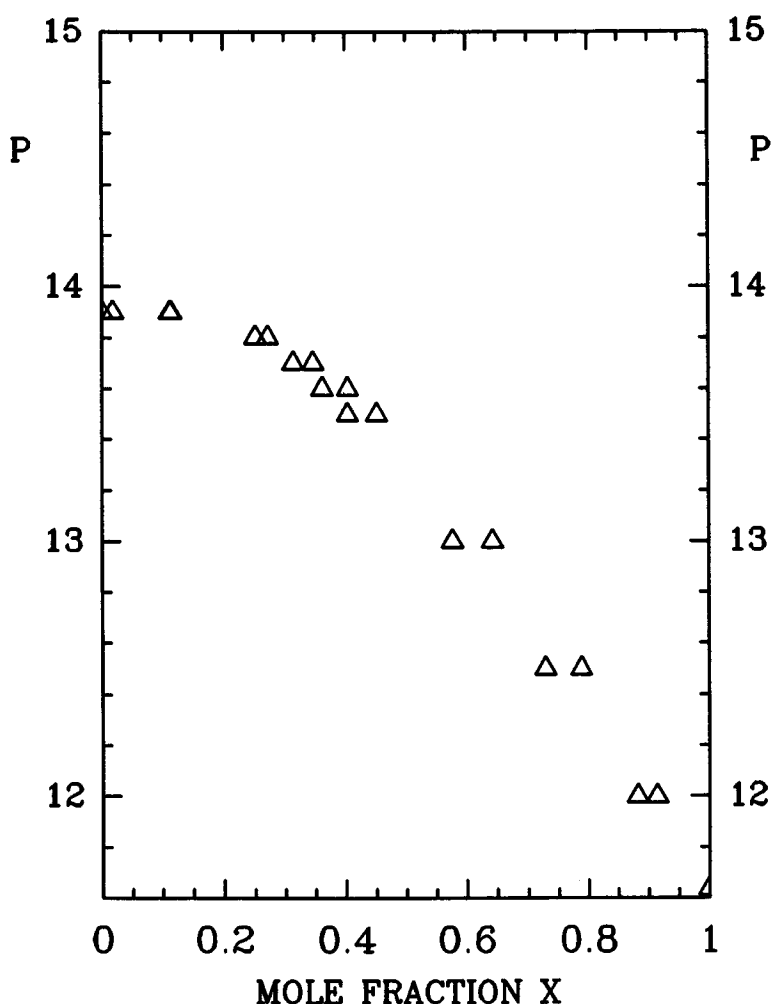
Figure 2.   Phase diagram of binary hard sphere mixture for diameter ratio $\alpha = 0.9425$. Triangles ($\triangle$) represent the computer simulation results. We estimate that for this value of α the nature of the phase diagram changes from spindle (figure 1) to azeotropic (figure 3). The pressure is expressed in units of $k_B T / \sigma_L^3$, where σ_L is the diameter of the larger sphere.

few striking differences between simulation and theory: first of all, the mole fraction of the large spheres of the eutectic point predicted by theory ($X \approx 0.08$), is much lower than the result of the computer simulation ($X \approx 0.26$). More seriously, we find in our computer simulations a small but non-negligible solubility of large spheres in a small sphere solid. Although we find a solubility of no more than 4%, density functional theory predicts a negligible solubility of large spheres in a small sphere matrix. According to Barrat et al. [5], the density functional prediction that the large spheres become insoluble in a matrix of small spheres for a diameter ratio of $\alpha = 0.85$ confirms the semi-empirical rule of Hume-Rothery [13] that no solid solutions can be formed by mixtures of particles with a diameter ratio smaller than 0.85. The present simulations do no support such a categorical statement, although the Hume-Rothery rule appears to be, at least qualitatively, correct.
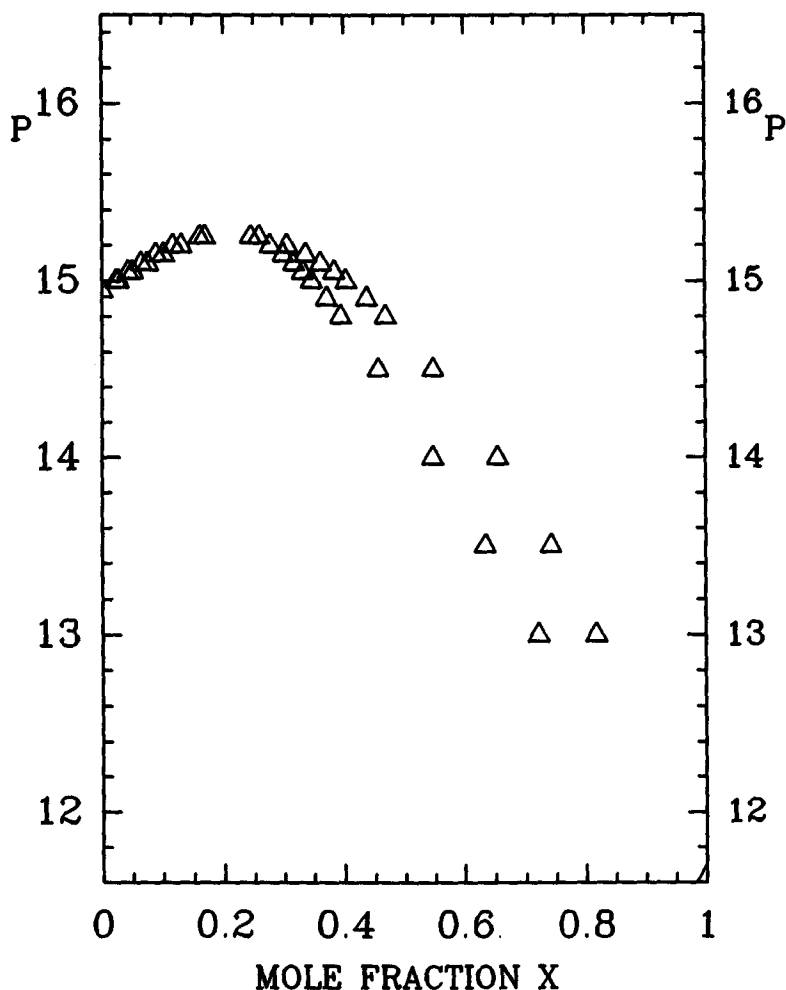
Figure 3. Azeotropic diagram of a binary hard sphere mixture for diameter ratio $\alpha = 0.92$. The triangles ($\triangle$) represent the computer simulation results. Note that Barrat *et al.* [5] predict a change from an azeotrope for $\alpha > 0.92$ to a eutectic for $\alpha < 0.92$. The pressure is expressed in units of $k_B T/\sigma_L^3$, where σ_L is the diameter of the larger sphere.

As the solubility of the large spheres in a solid matrix of small spheres is an important property of mixtures of dissimilar spheres, we have also estimated this solubility by a different method, namely by calculating the amount of reversible work needed to substitute a single large sphere in an array of small spheres.

The idea behind this calcuation is the following: very close to $X = 0$, the Gibbs free energy of the mixture must be of the form

$$G(X) = G_{\text{mono}} + X \ln X + (1 - X) \ln (1 - X) + aX,$$

where aX is the excess Gibbs free energy. We have used the fact that for small X, G_{ex} is linear in X. The constant a is determined in the following way: we compute the reversible work required to transform one sphere in a monodisperse FCC lattice into a larger sphere. In practice, we start with a 108-sphere FCC lattice and compute the reversible work needed to make this a mixture of 107 'small' spheres and one 'large'
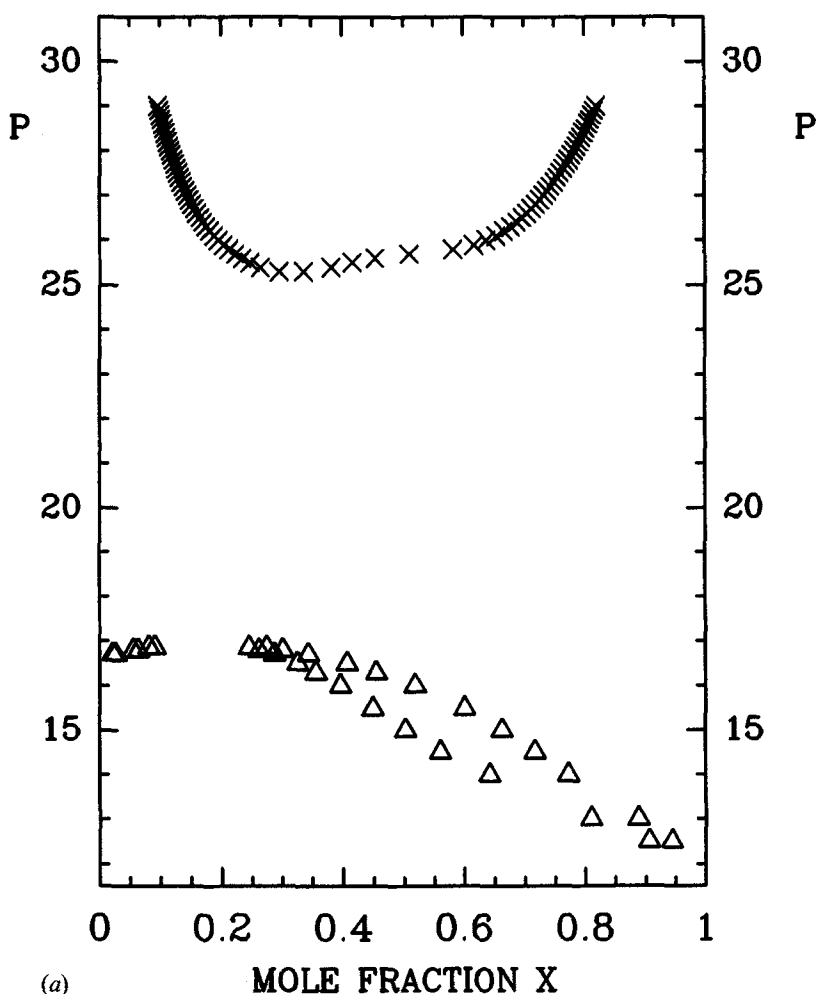
Figure 4.   Phase diagram of a binary hard sphere mixture for a diameter ratio $\alpha = 0.90$. For the sake of clarity the predictions of density functional theory and the simulation results have been drawn in two separate figures: (*a*) results obtained from computer experiments ($\triangle$); (*b*) theoretical prediction of Barrat *et al.* [5]. Note that the simulations indicate the presence of an azeotropic point, whereas the theory predicts eutectic behaviour. At pressures above $P = 25$, solid–solid demixing is observed ($\times$).

sphere, at constant packing fraction, and then compute the reversible work required to restore this 107 : 1 solid solution to the same pressure as the monodisperse system. Clearly, the larger is a, the less is the solubility of the large spheres in a matrix of small ones. If we use our 'measured' value for a to estimate the composition of the solid solution in equilibrium with the fluid, we find for $\alpha = 0.85$ and $P = 23.4$ (i.e. just above the eutectic pressure) that the mole fraction of large spheres in solid solution is $X \approx 0.08$. This is almost a factor of two larger than our best estimate for the composition of the solid at melting (see figure 6). However, this discrepancy is not surprising, because we computed a for $X = 1/108 \approx 0.9\%$, and we should not expect a linear extrapolation to hold all the way up to $X = 0.08$. The main conclusion that we base on the above test is that solubility of 4% large spheres in a solid matrix of small spheres is not excessive when compared with the limiting behaviour of G_{ex} for
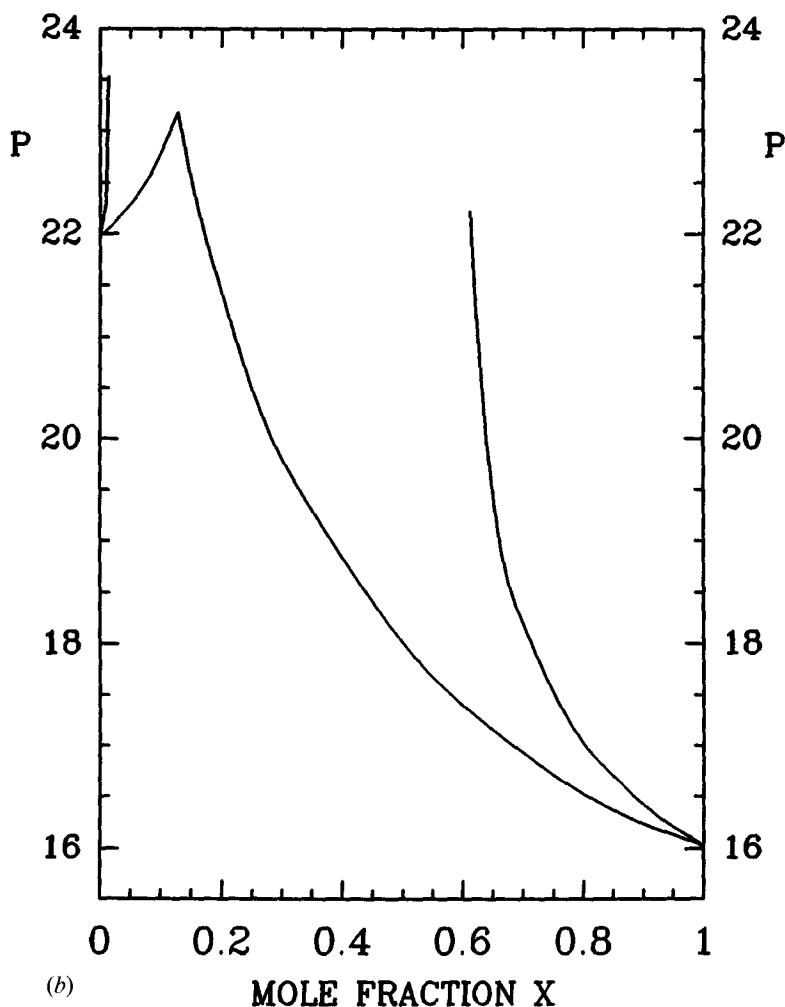
(b)

Figure 4 *(continued)*.

$X \to 0$. It is perhaps worth pointing out that the estimated mole fraction X of the (metastable) liquid is $X = 0.31$, which is in excellent agreement when we compare it with the phase diagram of 0.85, after extrapolation of the liquid branch of the low mole fraction X.

Continuing the comparison of computer simulation and theoretical predictions for $\alpha = 0.85$, we note that the solubility of small particles in a solid of large particles, as found in the simulation, is much smaller than predicted by density functional theory. However, on a qualitative level there is one feature that is correctly predicted by density functional theory, namely that the solidus branch for the solid that is richer in large spheres has a point where the solubility of the smaller spheres is maximum. Figure 6 shows that for coexistence pressures higher than approximately $P_{coex} = 18$ the solubility of small spheres decreases with increasing coexistence pressures, up to the eutectic point. This is not peculiar to hard spheres. Hume-Rothery and co-workers [13] pointed out that the same effect also occurs in some binary alloys, especially when the melting temperature of one of the components differs strongly from the temperature of the eutectic point.
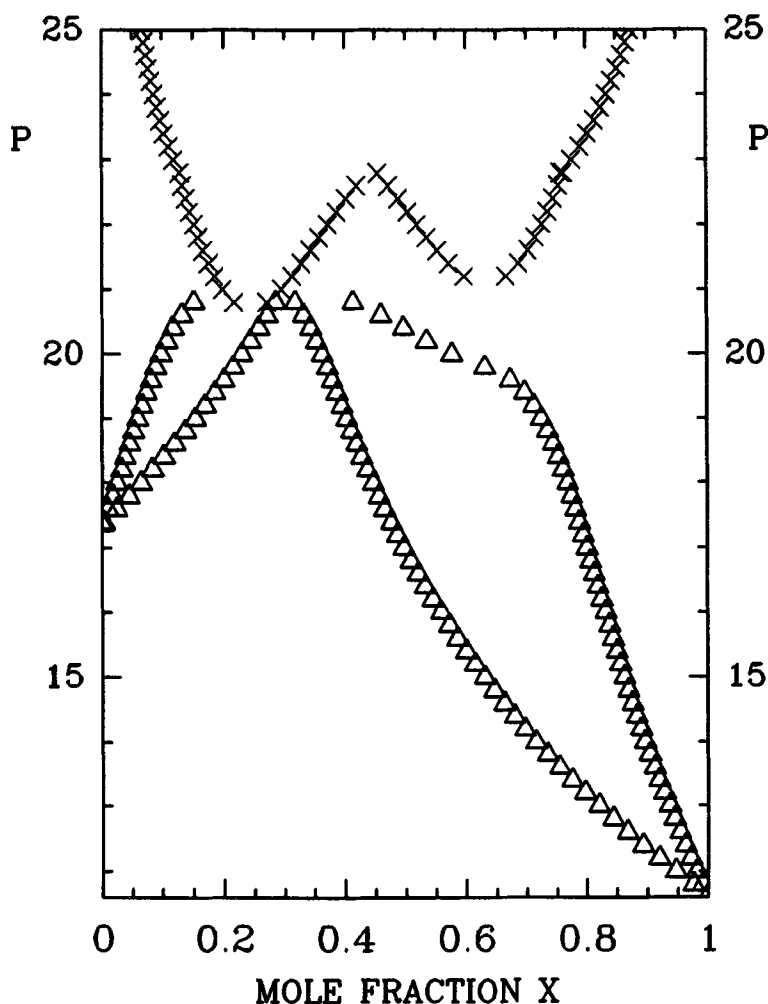
Figure 5.   Phase diagram of a binary hard sphere mixture for a diameter ratio $\alpha = 0.875$, as obtained from the present computer experiments. Triangles ($\triangle$) represent the liquid–solid transition, while ($\times$) crosses represent the solid–solid demixing. The pressure P is defined as in figure 1. Close to this value of α the azeotropic diagram (for $\alpha > 0.875$) changes into a eutectic (for $\alpha < 0.875$).

Using the analytical fits to the computer simulation data, we can predict the phase behaviour of hard sphere mixtures for diameter ratio other than 0·85, 0·90 and 0·95. By plotting phase diagrams for a range of diameter ratios, we find that the spindle diagram turns into an azeotrope at $\alpha = 0.9425$ (figure 2). This observation is in essentially perfect agreement with the prediction of density functional theory ($\alpha = 0.94$) [5].

Decreasing the diameter ratio, we start to find solid–solid phase separation in the pressure region studied. In figure 4 we have plotted the low-pressure part of the solid–solid coexistence curve. Note that the two-phase region is slightly asymmetric: there is always a minimum for low mole fractions of large spheres, and the solubility of the large spheres in a matrix of small spheres is always smaller than that of small spheres in a large sphere matrix, just as in the eutectic diagram of figure 6. Furthermore, even for the diameter ratio $\alpha = 0.90$ there is a considerable 'gap' between the
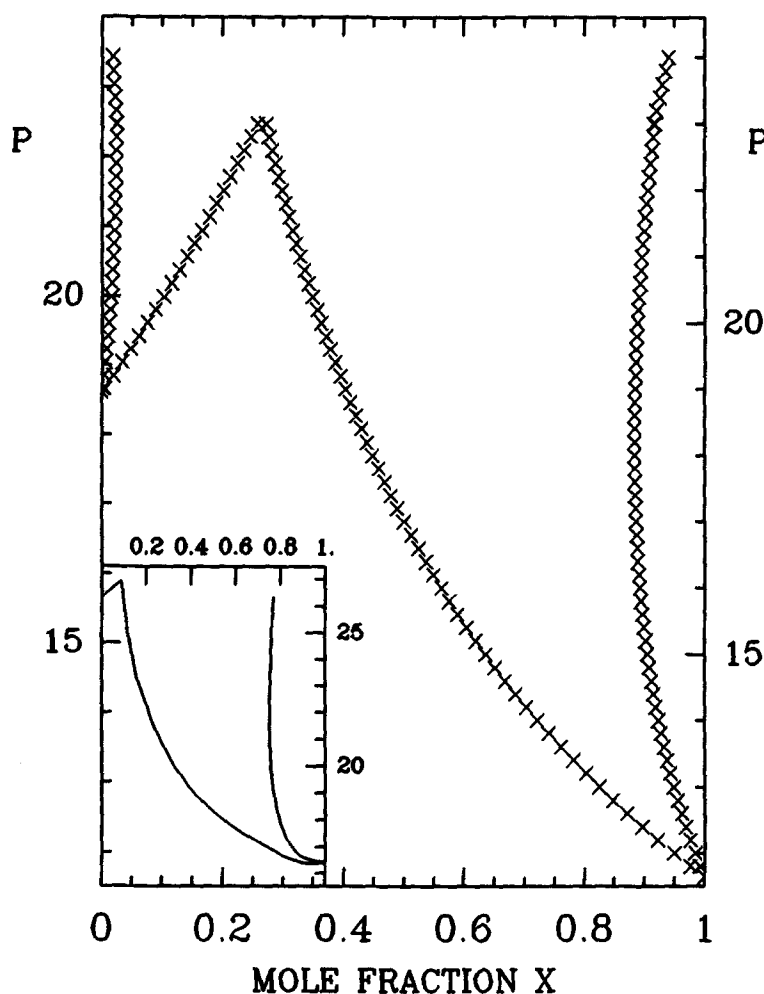
Figure 6. Phase diagram of a binary hard sphere mixture for a diameter ratio $\alpha = 0\cdot85$. For the sake of clarity the predictions of density functional theory and the simulation results have been drawn separately: the main diagram shows the results obtained from computer experiments (●); the inset in the corner shows the theoretical prediction of Barrat *et al.* [5]. Note that the computer experiments find a finite solubility for the larger spheres, whereas density functional theory predicts that this solubility is negligible.

pressure of the azeotropic point and the minimum of the solid–solid coexistence curve. Note that at this value of α density functional theory already predicts an eutectic diagram. A eutectic can only be formed in the solid–solid coexistence curve crosses the solid–liquid curve. This happens at a diameter of $\alpha = 0\cdot875$ (figure 5).

For this diameter ratio ($\alpha = 0\cdot875$ the solid–solid coexistence curve shows *two* minima. This suggest that a relatively stable solid mixture is formed —possibly a locally ordered structure with about equal mole fractions of large and small spheres. However, at present, we have no direct evidence to support this conjecture.

The question as to which crystal structure for the monodisperse hard sphere system—FCC or HCP—is thermodynamically the most stable is a long-standing problem. Early investigations [14, 15] already indicated that the difference in free

energy between both structures is extremely small. The most accurate calculations of the free energy difference were performed by Frenkel and Ladd [11]. These simulations only confirmed that the free energy difference between FCC and HCP is very small. In fact, in [11] it was found that this free energy difference was zero within the statistical uncertainty of the simulation ($0.002kT$ per particle at a packing fraction $\phi = 0.545$).

It is natural to ask how this free energy difference will depend on the diameter ratio for a binary mixture in a substitutionally disordered crystal. Therefore we also performed simulations for the HCP lattice.

We compared equimolar substitutionally disordered HCP and FCC crystals, composed of 108 particles in an orthorhombic box. For both crystals, the spheres were stacked in six closed packed planes, consisting of 3×6 particles. Both crystals were expanded from a packing fraction $\phi = 0.597$, and the equation-of-state data were calculated by MD simulations, starting at $\phi = 0.597$ down to the density where the crystals became mechanically unstable. Furthermore, we calculated additional equation-of-state data increasing packing fraction by compressing the crystals with NPT–MC. In this case we started from a well-equilibrated configuration at $\phi = 0.56$. For both HCP and FCC crystals the equation-of-state data obtained by MC reproduce the MD results very well, except at the highest packing fractions (above $\phi = 0.59$), where the acceptance of particle interchanges drops below 1%.

The results of both methods indicate that for low packing fractions (below $\phi = 0.58$) the equations of state of both crystal structures are indistinguishable, whereas for higher packing fractions the pressure of the HCP crystal is slightly higher. This suggests that at higher packing fractions the FCC phase becomes slightly more favoured than the HCP crystal, where we have used the fact that the difference in free energy of both crystal structures close to the melting point is negligible.

3.2. Thermodynamic properties at coexistence

Another quantity that can be compared with the prediction of density functional theory [5] is the packing fraction of the liquid ϕ_f and solid ϕ_s at coexistence.

Figures 7 and 8 give the packing fractions at coexistence for the liquid and solid state. The squares in figure 7 displays the packing fractions for both solid curves of the eutectic diagram of figure 6, while the squares in figure 8 shows the packing fractions for the liquid ending up in the eutectic point.

The ratio $(\phi_s - \phi_f)/\phi_f$ is plotted in figure 9–11 as a function of the mole fraction X. For all diameter ratios the theoretical predictions differ from the results of the computer simulations. One could expect such a discrepancy for the freezing of systems with a diameter ratio $\alpha = 0.90$ and 0.85: for $\alpha = 0.90$ (figure 10) even the qualitative theoretical prediction of the liquid–solid diagram is wrong (figure 4), and although the theoretical prediction of an eutectic diagram in the case of $\alpha = 0.85$ is correct, a number of quantitative differences between the phase diagrams obtained from the theory and computer simulation were found (see figure 6).

This discrepancy is quite pronounced for $\alpha = 0.95$ (figure 9): instead of a maximum as predicted by density functional theory, we find a *minimum* for $(\phi_s - \phi_f)/\phi_f$. Note that the prediction of the density functional theory of [5] for the relative density difference at coexistence is already apparently higher for the monodisperse case.

3.3. Discussion

One may wonder to what extent our simulation results for relatively small systems (108 particles) are representative of the phase behaviour in the thermodynamic limit.
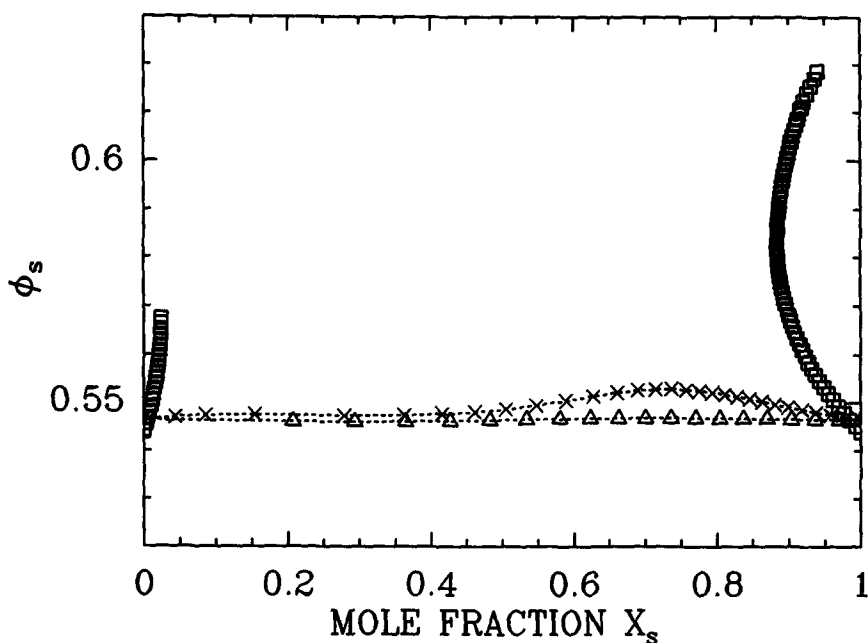
Figure 7. Packing fractions ϕ_s of the solid at coexistence of the liquid–solid transition versus the mole fraction of the large spheres in the solid, denoted by X_s. The different diameter ratios are shown: $\alpha = 0.95$ ($\triangle$), 0.90 (×) and 0.85 ($\square$). The dotted lines serve as a guide to the eye.

For the sake of clarity we first discuss the influence of statistical and systematical errors on the individual phase diagrams, and thereafrer we give an argument why the determination of the estimated diameter ratios at which the phase diagrams change in character (spindle → azeotrope, azeotrope → eutectic) will depend only slightly on system size.

Statistical and systematic errors directly influence the individual phase diagrams: the random errors originate from statistical noise in our simulations, while the systematic errors originate from the influence of system size, periodic boundary conditions etc.

The statistical errors in the free enthalphy for both the liquid and the solid are estimated to be between 1 and 2%. This estimate is based on the relative error of about 1% in the thermodynamic properties, directly obtained from MD and MC simulations. To test the stability of our results against statistical fluctuations, we have calculated the phase diagrams with different subsets of our simulation data and with different numbers of terms in the polynomial fit. Choosing quite different subsets of simulation data or varying the number of terms in the polynomial fit hardly changes the features of the phase diagrams: only small shifts are observed. The small influence of the changes of the data set is plausible when one takes into account that our basic data set (i.e. the one from which the phase diagrams in figures 1–6 were calculated) consisted of about 1200 data points. This large number allows one to leave out a considerable number of data from the basic data set, while still keeping a good estimate of the individual phase diagrams.
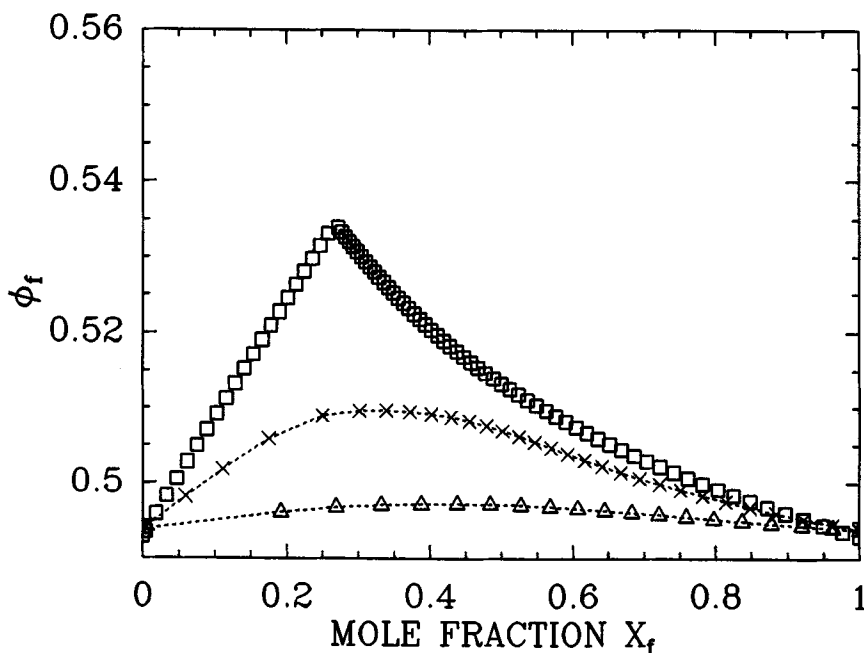
Figure 8.   Packing fraction ϕ_f of the liquid at coexistence of the liquid–solid transition versus the mole fraction of the large spheres in the liquid, denoted by X_f. Three different diameter ratios are shown: $\alpha = 0.95$ ($\triangle$), 0.90 (×) and 0.85 ($\square$). The dotted lines serve as a guide to the eye.

Although the qualitative features of the phase diagrams are not strongly influenced by statistical fluctuations in our data, some quantitative features are sensitive to these fluctuations. In particular, we have investigated the eutectic point for $\alpha = 0.85$ for a different number of terms in the polynomial fit. Comparing the results of fits with 12 terms and 32 terms, the mole fraction x of the eutectic point shifted from $X \approx 0.26$ to $X = 0.30$, indicating that this quantity is relatively sensitive to small changes in the data. Note, however, that density functional theory predicts $X \approx 0.08$ for the eutectic point, still more than three times lower than we find with different numbers of terms.

To study the consequences of the systematic errors, it is useful to compare the binary systems with the monodisperse system. For the monodisperse system Hoover and Ree have studied the limit to the infinite system for the liquid and the solid. For the liquid the system-size dependence can be estimated from the virial expansion, for which the system-size dependence of the virial coefficients can be calculated as an asymptotic expansion under periodic boundary conditions [16]. For a monodisperse system of 108 spheres the system-size dependence of the compressibility factor ranges from approximately 1% at low densities to 2% at high densities [17]. For diameter ratios near the monodisperse limit the compressibility factor of the liquid hardly depends on the composition for these diameter ratios [9]. Thus it is assumed that the virial coefficients hardly depend on the composition for these diameter ratios either, which can be verified explicitly for the second and third virial coefficients [18]. Because of the small differences between the mixture and the monodisperse system for the diameter ratios studied in this paper, we expect the same system-size dependence for these mixtures as for the monodisperse system.
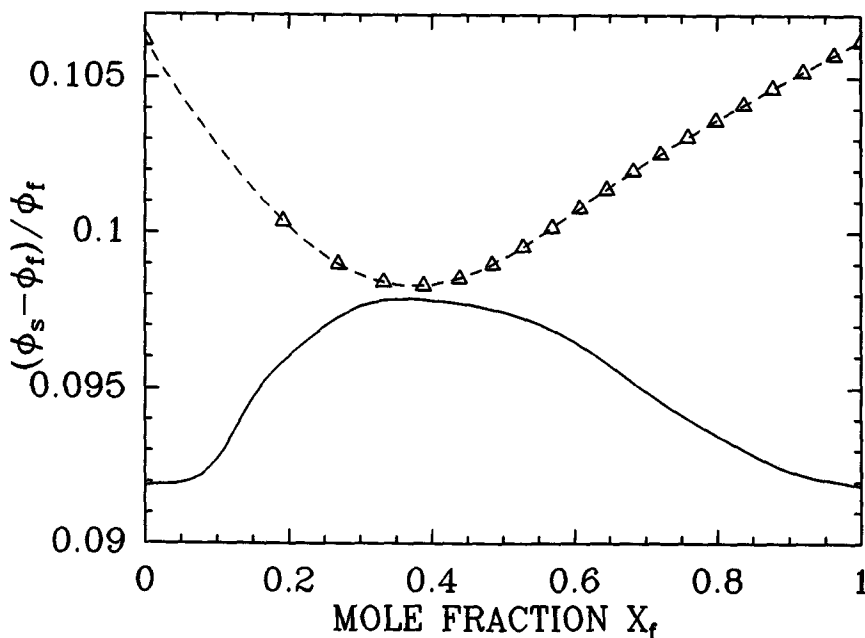
Figure 9.   Relative difference in the packing fraction at phase coexistence as a function of the mole fraction of the large spheres in the liquid, denoted by X_f, for a binary hard sphere mixture with diameter ratio $\alpha = 0.95$. ϕ_s is the packing fraction of the solid and f_f that of the liquid. The solid line is the theoretical prediction of [5]. The computer simmulation data are represented by triangles ($\triangle$). The dashed curve is drawn as a guide to the eye.

Unfortunately, for the solid state we cannot make use of arguments based on asymptotic expansion analysis.

For a monodisperse system Wood and Salsburg [19] derived an asymptotic expansion for the system-size dependence of an ordered crystal in the neighbourhood of closest packing. To first order in $\rho_0/\rho - 1$, where ρ_0 in the density of closest packing, they found a $(N - 1)/N$ dependence for the compressibility of the system. This result was derived under the assumption of periodic boundary conditions. Hoover and Ree showed that this approximation still holds near liquid–solid coexistence. However, for substitutionally disordered crystals there is no obvious definition of the density of closest packing. If we assume the same system-size dependence for the disordered as for the ordered system, we may estimate the systematic error to be 1%. Owing to the large amount of data, it is practically impossible to check the system-size dependence of the pressure for all compositions and diameter ratios. However, we have tested this assumption by making a few random checks. For $\alpha = 0.85$ we compared systems consisting of 108 and 256 particles of an equimolar solid ($X = 0.5$). Results are displayed in the table, from which it can be seen that, on increasing the system size from 108 to 256 particles, the systematic error is of the order of 1%. Furthermore, as was pointed out before, the statistical error in our data is of the same order of magnitude as the systematic error. So, by testing the influence of the statistical error, we also probe the sensitivity of our results to small systematic errors.

An independent argument for the small influence of the systematic errors is the fact that the coexistence pressure of the liquid–solid transition of the monodisperse
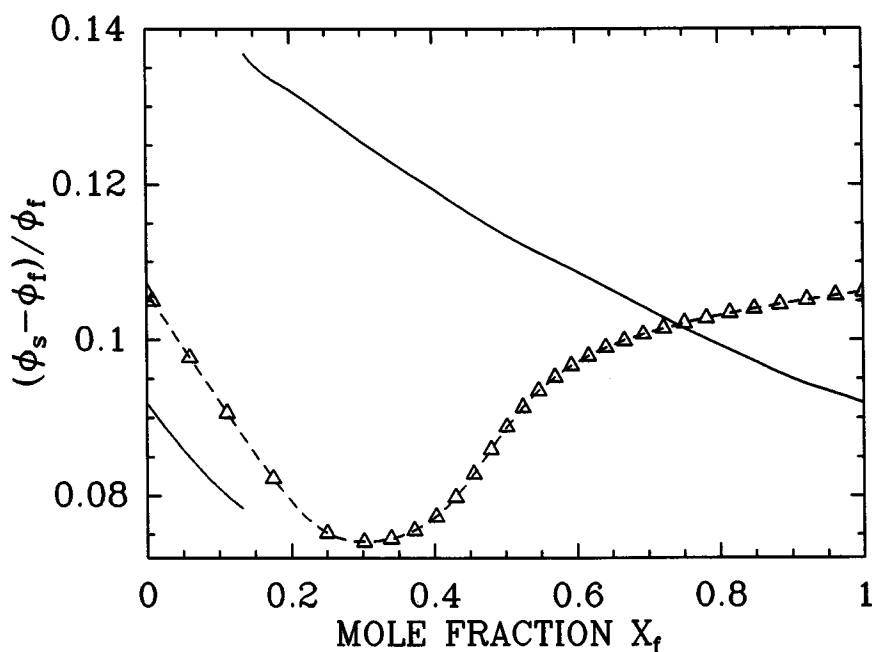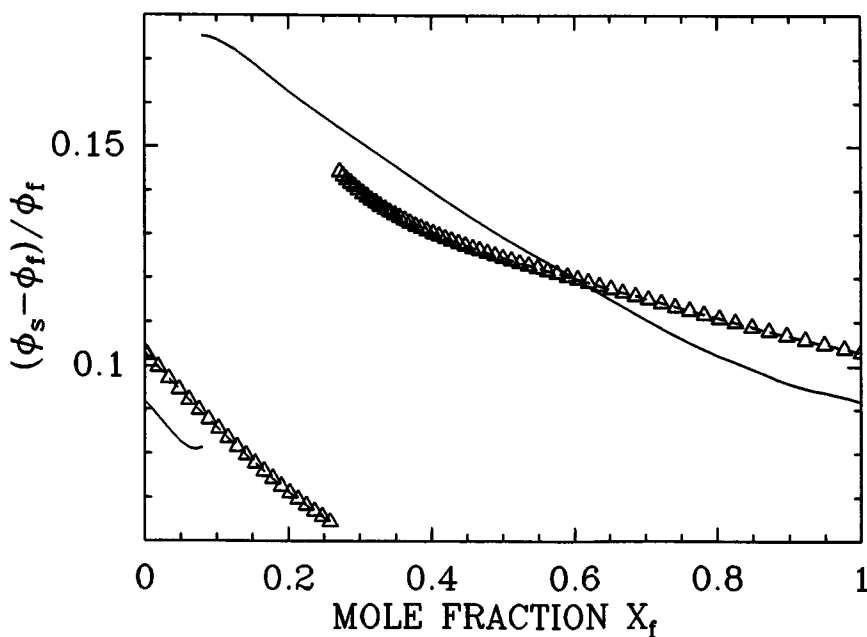
Figure 10.　Relative difference in the packing fraction at phase coexistence as a function of the mole fraction of the large spheres in the liquid, denoted by X_f, for a binary hard sphere mixture with diameter ratio $\alpha = 0.90$. See figure 9 for definitions of symbols and lines.

Figure 11.　Relative difference in the packing fraction at phase coexistence as a function of the mole fraction of the large spheres in the liquid, denoted by X_f, for a binary hard sphere mixture with diameter ratio $\alpha = 0.85$. See figure 9 for definitions of symbols and lines.

System-size dependence of the pressure in a binary hard sphere mixture, obtained from MD
simulations. The results refer to substitutionally disordered crystals at a diameter ratio
$\alpha = 0.85$.

	$X = 0.5$	
ρ	108	256
1·065	17·41(10)	17·24(5)
1·0775	18·95(7)	18·41(4)
1·09	19·98(9)	20·07(6)
1·10	21·49(17)	21·61(6)

system, as estimated from our data set of 1200 data, deviates less than 1% from the
coexistence pressure obtained by Hoover and Ree by taking the limit to an infinitely
large system [3]. We conclude that there are no indications for a strong influence of
the statistical and systematic errors on the qualitative features of the phase diagrams.

Finally, it is easy to understand that our estimate of the diameter ratios, for which
the spindle diagram changes over to an azeotropic and the azeotropic to an eutectic
diagram, will not be very sensitive to errors in the data. Consider, for instance, the
changeover from the azeotropic to the eutectic diagram (which is estimated for
$\alpha = 0.875$, figure 5). If we now change our data set or use a different number of terms
in our polynomial fit, this will cause a small change of the calculated phase diagrams.
This small change of the quantitative features of the phase diagrams can also be
obtained approximately, when we use our original polynomial fit, but with a slightly
different diameter ratio. Comparing the phase diagrams for $\alpha = 0.90$ and 0.875
(figures 4 and 5) shows that even a small change in the diameter ratio α of 0.025 has
a drastic influence on the quantitative features of the phase diagram. This means that
the small changes of the phase diagram, which we observe when we use different data
sets, should be equivalent to very small changes in the diameter ratios. From the
different data sets and polynomial fits that we have tested, we estimate the uncertainty
in the diameter ratio for the azeotropic–eutectic change to be approximately
$\Delta\alpha = 0.005$.

4. Summary and conclusions

We have presented the phase diagrams of binary hard-sphere mixtures in the range
of diameter ratios $0.85 \leqslant \alpha \leqslant 1.00$, assuming that the solid is a substitutionally
disordered lattice, i.e. a solid solution. These results have been compared with those
of the density functional theory of Barrat *et al.* [5].

We have found three types of phase diagrams in the range of diameter ratios
$1.00 \geqslant \alpha \geqslant 0.85$: a spindle, an azeotrope and a eutectic diagram, in this order for
decreasing diameter ratio. The change from a spindle diagram to an azeotrope occurs
at a diameter ratio of $\alpha = 0.9425$ (as predicted by density functional theory [5] and
the change from an azeotrope to a eutectic diagram at $\alpha = 0.875$ (in disagreement
with the predictions of [5]).

When we compare these phase diagrams with the results of one version of density
functional theory, we conclude that this theory predicts the spindle diagram for
$\alpha = 0.95$ correctly, but for $\alpha = 0.90$ its prediction of an eutectic diagram is in conflict
with the axeotropic diagram, found in the computer calculations. Both density
functional theory and computer simulations do find a eutectic diagram for $\alpha = 0.85$.
However, the computer experiments show that the solubility of large spheres in a

matrix of small spheres is finite, whereas density functional theory predicts that this solubility is negligible.

For the phase diagram of $\alpha = 0.875$ we have found that the solid–solid coexistence curve contains two minima. This suggests that a second stable solid phase can be formed beside the substitutionally disordered solid.

Whereas there is a qualitative agreement between the phase diagrams predicted by density functional theory and calculated by computer simulations, there is a failure of this theory to predict the difference in packing fraction between the solid and the liquid: the most remarkable example is for the system with diameter ratio $\alpha = 0.95$: computer simulations find a minimum in the relative difference, in contrast with the maximum predicted by theory.

It would be interesting if the recent advances in the density functional theory of monatomic solids could be extended to binary mixtures. A comparison between such a density functional theory and the present simulation results would allow us to decide whether the discrepancies between the current second-order density functional theories and our simulations are merely due to the same approximations that spoil the agreement between the second-order density functional theory and simulations for monodisperse systems, or that the reasons for the shortcomings of DFT for binary mixtures have deeper, as yet unknown causes.

Addendum

After this manuscript was completed, we received preprints from Zeng and Oxtoby [20] and Denton and Ashcroft [21] describing improved density functional theories of the melting behaviour of binary hard sphere mixtures. Although the theoretical approaches in [20, 21] are different, both groups arrive at very similar theoretical predictions, which are, moreover, in good agreement with the simulation data reported in the present paper.

References

[1] BAUS, M., 1987, *J. statist. Phys.*, **48**, 1129; 1990, *J. Phys. cond. Matter*, **2**, 2111.
[2] BAUS, M., and COLOT, J. L., 1985, *Molec. Phys.*, **55**, 653.
[3] HOOVER, W. G., and REE, F. H., 19068, *J. chem. Phys.*, **49**, 3609.
[4] LUTSKO, J. F., and BAUS, M., 1990, *Phys. Rev. Lett.*, **64**, 761.
[5] BARRAT, J. L., BAUS, M., and HANSEN, J. P., 1986, *Phys. Rev. Lett.*, **56**, 1063; 1987, *J. Phys.* C **20**, 1413.
[6] SMITHLINE, S. J., and HAYMET, A. D. J., 1987, *J. chem. Phys.*, **86**, 6486; 1988, *J. chem. Phys.*, **88**, 4104; RICK S. W., and HAYMET, A. D. J., 1989, *J. chem. Phys.*, **90**, 1188.
[7] JACKSON, G., ROWLINSON, J. S., and VAN SWOL, F., 1987, *J. phys. Chem.*, **91**, 4907.
[8] KRANENDONK, W. G. T., and FRENKEL, D., 1989, *J. Phys. cond. Matter*, **1**, 7735.
[9] KRANENDONK, W. G. T., and FRENKEL, D., 1991, *Molec. Phys.*, **72**, 715.

[10] FRENKEL, D., 1986, *Molecular Dynamics Simulations of Statistical Mechanical Systems: Proceedings of the International School of Physics 'Enrico Fermi'*, Course XCVII, edited by G. Ciccotti and W. G. Hoover (North-Holland), p. 156.

[11] FRENKEL, D., and LADD, A. J. C., 1984, *J. chem. Phys.*, **81**, 3188.

[12] KRANENDONK, W. G. T., and FRENKEL, D., 1991, *Molec. Phys.*, **72**, 699.

[13] HUME-ROTHERY, W., SMALLMAN, R. E., and HAWORTH, C. W., 1966, *The Structure of Metals and Alloys* (The Metals and Metallurgy Trust).

[14] ALDER, B. J., HOOVER, W. G., and YOUNG, D. A., 1968, *J. chem. Phys.*, **49**, 3688.

[15] ALDER, B. J., CARTER, B. P., and YOUNG, D. A., 1969, *Phys. Rev.*, **183**, 831.

[16] SALSBURG, Z. W., 1966, *J. chem. Phys.*, **44**, 3090; 1966, *J. chem. Phys.*, **45**, 2719.

[17] ERPENBECK, J. J., and WOOD, W. W., 1984, *J. statist. Phys.*, **35**, 321.

[18] MCLELLAN, A. G., and ALDER, B. J., 1956, *J. chem. Phys.*, **24**, 115.

[19] SALSBURG, Z. W., and WOOD, W. W., 1962, *J. chem. Phys.*, **37**, 798.

[20] ZENG, X. C., and OXTOBY, D. W., 1990 *J. chem. Phys.*, **93**, 4357.

[21] DENTON, A. R., and ASHCROFT, N. W., Preprint.